Interaction between G-Actin and Various Types of Liposomes: A ^{19}F, ^{31}P, and ^{2}H Nuclear Magnetic Resonance Study†

Mario Bouchard,‡ Chantal Paré,‡ Jean-Pierre Dutasta,§ Jean-Paul Chauvet,§ Claude Gicquaud,|| and Michèle Auger*,‡

Département de Chimie, CERSIM, Université Laval, Québec, Québec, Canada G1K 7P4, Stéréochimie et Interactions Moléculaires, École Normale Supérieure de Lyon, 69364 Lyon Cedex 07, France, and Département de Chimie-Biologie, Université du Québec à Trois-Rivières, Trois-Rivières, Québec, Canada G9A 5H7

Received August 1, 1997; Revised Manuscript Received December 16, 1997

ABSTRACT: We have investigated in the present study the interaction between G-actin and various types of liposomes, zwitterionic, positively charged, and negatively charged. To investigate at the molecular level the conformation of actin in the presence of lipids, we have selectively attached a fluorinated probe, 3-bromo-1,1,1-trifluoropropanone, to the actin cysteine residues 10, 285, and 374 and used high-resolution ^{19}F nuclear magnetic resonance spectroscopy to investigate the probe resonances. The results indicate a change in the mobility of the ^{19}F labels when G-actin is in the presence of positively charged liposomes made of DMPC and stearylamine and in the presence of DMPG, a negatively charged lipid. No conformational change was observed in the actin molecule in the presence of neutral liposomes. Electron micrographs of these systems reveal the formation of paracrystalline arrays of actin filaments at the surface of the positively charged liposomes, while no evidence of actin polymerization or paracrystallization was observed in the presence of DMPG. The interaction between actin and the lipid polar headgroup has also been investigated using solid-state phosphorus and deuterium NMR. The results indicate no evidence of interaction between actin and zwitterionic liposomes but show an interaction between the positively charged liposomes and a negative charge on the actin molecules. Interestingly, the negatively charged liposomes interact with a positive charge, which is most likely associated with the three residues (His-Arg-Lys) preceding the cysteine 374 residue in the protein.

Actin is a ubiquitous cytoskeletal protein which is involved in cell motility and morphogenesis. At low ionic strength, actin is a ~43 kD monomer named G-actin because of its globular shape. As the ionic strength is increased to the physiological level, G-actin polymerizes into thin filaments called F-actin. During the polymerization process, the ATP molecule bound to actin is hydrolyzed to ADP[1] (*1*).

Numerous studies have focused on elucidating the exact nature of the actin/membrane interaction. Most evidence supports the idea that actin interacts with membranes via other proteins. That is, actin filaments are believed to be anchored to the membrane through actin-binding proteins. Most likely candidates include integral membrane proteins such as ponticulin in *Dictyostelium* (*2*), myosin I (*3*), and hisactophilin (*4*). Alternatively, the attachment has been proposed to occur via a multi-protein network involving spectrin/fodrin (*5*), protein 4.1 (*6*), α-actinin (*7*), vinculin (*8*), and talin (*9*).

However, our group has shown that actin can also interact directly with lipids without the need of an intermediate linker protein (*10*−*14*) using an in vitro system composed of pure lipids and purified actin (*12*). Electron microscopy and differential scanning calorimetry (DSC) analysis have shown changes in actin conformation upon interaction with membrane lipids (*13*). The interaction has been shown to occur with positively charged lipids or zwitterionic lipids in the presence of millimolar concentrations of divalent cations which may be either calcium or magnesium. Therefore, the mechanism of the interaction seems to be electrostatic in nature. On the other hand, it has been shown using high-pressure FTIR spectroscopy that during this interaction, the actin molecules, rich in β-sheets, seem to be stabilized by the interaction with the membrane but that the lipid organization of the membrane is not significantly affected by the interaction with actin (*14*).

Skeletal muscle actin contains five cysteine residues in a sequence of 375 amino acids (*15*). These occur at positions 10, 217, 257, 285, and 374 (*15*−*17*). Actin can be selectively alkylated using 3-bromo-1,1,1-trifluoropropanone (BTFP) at cysteines 10, 285, and 374. Cysteine 374 is the most reactive, and cysteines 10 and 285 can be alkylated to a lesser extent under relatively native conditions (*18*−*20*).

† This work was supported by the Natural Science and Engineering Research Council (NSERC) of Canada, by the Fonds pour la Formation de Chercheurs et pour l'Aide à la Recherche (FCAR) from the Province of Québec and by the Ministère de l'Enseignement Supérieur et de la Science of the Province of Québec.

* Author to whom correspondence should be addressed at Département de Chimie, CERSIM, Université Laval, Québec, Québec, Canada G1K 7P4. Telephone: 418-656-3393. Fax: 418-656-7916. E-mail: Michele.Auger@chm.ulaval.ca.

‡ Université Laval.

§ École Normale Supérieure de Lyon.

|| Université du Québec à Trois-Rivières.

[1] Abbreviations: ADP, adenosine diphosphate; ATP, adenosine triphosphate; BTFP, 3-bromo-1,1,1-trifluoropropanone; DMPC, dimyristoylphosphatidylcholine; DMPG, dimyristoylphosphatidylglycerol; DSC, differential scanning calorimetry; FTIR, Fourier transform infrared; NMR, nuclear magnetic resonance; SA, stearylamine; TFA, trifluoroacetic acid.

S0006-2960(97)01892-8 CCC: $15.00
Published on Web 02/11/1998

In the present study, we have used ^{19}F nuclear magnetic resonance spectroscopy, in conjunction with ^{19}F labeling, to study at a molecular level the effect of different types of liposomes, zwitterionic or charged, on the environment of the cysteine residues 10, 285, and 374 of G-actin. ^{19}F NMR has proven to be a useful probe to study the conformation and mobility of proteins (*18, 19, 21, 22*). It offers the advantages of high sensitivity, a wide chemical shift range, and 100% natural abundance. Moreover, since ^{19}F is not naturally occurring in proteins, there is no background resonance, which therefore simplifies the interpretation of the spectra.

Since actin is most likely to interact with the lipid headgroup, we have also investigated the interaction using ^{31}P and ^{2}H solid-state NMR. ^{31}P NMR is a valuable tool to investigate the phase of the different systems studied. On the other hand, ^{2}H NMR of the phosphatidylcholine headgroup has been widely used to examine electrostatic interactions between charged species and a membrane surface (*23*−*30*). The bilayer surface charges induce a conformational change in the headgroup of certain phospholipids, and in phosphatidylcholine the $P^{-}-N^{+}$ dipole of the choline headgroup appears to realign under the influence of a surface electrical field. If the headgroup is specifically deuterated, the conformational change alters the measured ^{2}H quadrupolar splittings in the ^{2}H NMR spectra. More specifically, it has been shown that counterdirectional changes in the magnitudes of the α and β deuteron quadrupolar splittings occur in response to changes in membrane surface charge density. In this respect, phosphatidylcholine is said to behave like a "molecular voltmeter" (*24*−*30*). This probe should therefore be very sensitive to the interaction between the negatively charged actin molecule and the lipid headgroup.

MATERIALS AND METHODS

Materials. Dimyristoylphosphatidylcholine (DMPC), dimyristoylphosphatidylglycerol (DMPG), and DMPC deuterated on the headgroup (DMPC-d_4) were purchased from Avanti Polar Lipids (Alabaster, AL) and used without any purification. Stearylamine was purchased from Sigma Chemical Co. (St. Louis, MO) and used without any purification. The following nomenclature is used to indicate deuteron positions in the phosphocholine headgroup:

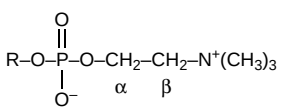

3-Bromo-1,1,1-trifluoropropanone (BTFP) was purchased from Aldrich Chemical Co. (Milwaukee, WI), and the salts used in the preparation of the buffer were of analytical grade.

Sample Preparation. Actin was extracted from rabbit muscle acetonic powder by the method of Spudich and Watts (*31*), modified by Nonomura et al. (*32*). Actin was obtained in the monomeric form and dissolved in a low ionic strength buffer (G buffer) made of 2 mM Tris-HCl, 0.2 mM ATP, 0.2 mM $CaCl_2$, 0.5 mM β-mercaptoethanol, and 0.01% sodium azide, pH 8.0. Actin polymerization was induced by 2 mM $MgCl_2$. Labeling of G-actin with 3-bromo-1,1,1-trifluoropropanone (BTFP) was achieved following the method of Brauer and Sykes (*18*).

Zwitterionic and negatively charged liposomes were made of dimyristoylphosphatidylcholine (DMPC) and dimyristoylphosphatidylglycerol (DMPG), respectively, whereas positively charged liposomes were prepared from a mixture of DMPC and stearylamine (9:1 molar ratio). For the ^{2}H NMR experiments, the negatively charged liposomes were prepared by mixing deuterated DMPC-d_4 in a 1:1 molar ratio with DMPG. The presence of deuterated DMPC was necessary as a probe for the molecular voltmeter effect. The same system (DMPC:DMPG, 1:1 molar ratio) was also used for the ^{31}P NMR experiments.

The lipid systems were codissolved in chloroform to ensure a homogeneous mixture. The organic solvent was evaporated with a nitrogen stream, followed by high vacuum overnight to ensure complete evaporation of the solvent. All liposome samples were directly hydrated with the G-actin solution. G-actin and liposomes were mixed at a 1:3 protein/lipid weight percent final concentration. The pH of all actin−liposome mixtures was adjusted to 8.0. Actin and liposomes were allowed to interact together for 1 h at room temperature prior to the NMR measurements.

^{19}F NMR spectroscopy. The ^{19}F NMR spectra were recorded on a Bruker AC-F 300 NMR spectrometer (Bruker Spectrospin, Milton, ON) operating at a frequency of 282.23 MHz for ^{19}F. A 90° pulse width of 8.0 μs was used with a repetition time of 1.1 s, of which 0.7 s was a preacquisition delay. The spectral width was set to 10 kHz, and 8K data points were recorded for each free induction decay. Chemical shifts were referenced relative to external trifluoroacetic acid (TFA) at 0 ppm. Negative upfield shifts from TFA were obtained for BTFP−G-actin. Samples were placed in 5 mm NMR tubes, and the spectra were recorded at room temperature (24 °C). For each spectrum 30 000 scans were acquired.

^{31}P NMR Spectroscopy. The ^{31}P spectra were acquired at 121.5 MHz on a Bruker ASX-300 (Bruker Spectrospin) operating at a ^{1}H frequency of 300.00 MHz. Experiments were carried out with a broad-band/^{1}H dual frequency 4 mm probe-head under conditions of proton decoupling. The free induction decays (2K data points) were recorded with a spin-echo sequence with a 4 s repetition time, a 90° pulse length of 5 μs, and an echo spacing of 30 μs. Between 6000 and 12000 decays were acquired for each spectrum. The temperature was controlled to within ±0.5 °C, and the chemical shifts expressed in parts per millions (ppm) were referenced relative to the signal of phosphoric acid at 0 ppm. A line broadening of 300 Hz was applied to all spectra.

^{2}H NMR Spectroscopy. The ^{2}H NMR spectra were recorded on a Bruker ASX-300 spectrometer (Bruker Spectrospin) operating at a ^{2}H frequency of 46.05 MHz. The spectra were recorded with a 10 mm static probe-head using a quadrupolar echo sequence (*33*) with a delay of 16 μs between pulses and a recycle delay of 500 ms. The 90° pulse length was 6 μs, and the sweep width was set to 100 kHz. Between 10 000 and 26 000 scans were acquired for each spectrum. A 200 Hz line broadening was applied to all spectra. To measure precisely the quadrupolar splittings associated with each deuteron in the ^{2}H spectra, the spectra that have an axially symmetric line shape were converted into ones that have the characteristics of 90° oriented samples using the dePaking technique (*34, 35*), resulting in better resolved spectra.

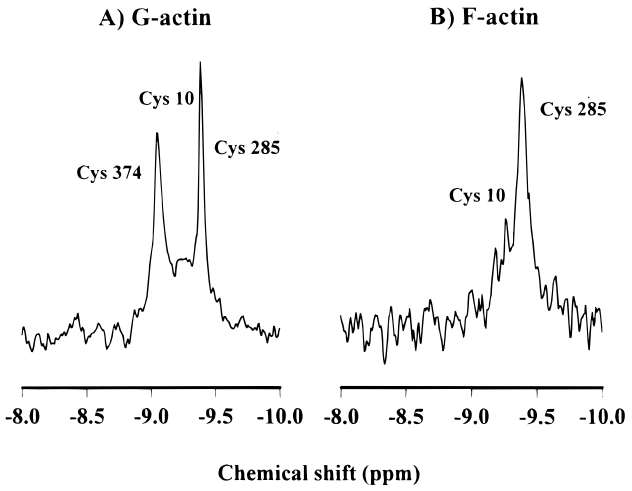

FIGURE 1: ^{19}F NMR spectra at 24 °C of native fluorinated (A) G-actin and (B) F-actin.

Electron Microscopy. The samples, prepared as indicated above, were incubated for 1 h at room temperature. The actin−liposome mixtures were then diluted in G buffer in order to get an actin concentration of 0.05 mg/mL. One drop of this suspension was put onto a Formvar-Carbon coated grid and negatively stained with 1% uranyl acetate in water.

RESULTS AND DISCUSSION

In the present study, we have first investigated by ^{19}F NMR spectroscopy the cysteine residues 10, 285, and 374 of pure ^{19}F-labeled actin in the monomeric form (G-actin) and in the polymerized form (F-actin). We have also investigated the interaction between G-actin and three different types of liposomes, zwitterionic, positively charged, and negatively charged. The complexes have been investigated both from the labeled actin point of view, using ^{19}F NMR spectroscopy, and from the lipid headgroup point of view, using ^{31}P and ^{2}H solid-state NMR spectroscopy. In addition, electron micrographs have been recorded for the complexes between actin and charged liposomes.

^{19}F NMR Spectroscopy of G- and F-Actin. Figure 1 shows the ^{19}F NMR spectra of native fluorinated G- and F-actin at room temperature. The ^{19}F NMR spectrum of pure BTFP−G-actin (Figure 1A) reveals broad resonances from the three labeled cysteine residues 10, 285, and 374 (*18, 19*). These results are in full agreement with those obtained by Brauer and Sykes (*18*). The two sharp resonances at −9.0 and −9.4 ppm can be assigned to the ^{19}F label attached to cysteines 374 and 285, respectively. The somewhat broader and less intense resonance at −9.3 ppm is assigned to the label attached to cysteine 10. Free labels were removed completely by extensive dialysis. When G-actin is polymerized to F-actin in the presence of 2 mM $MgCl_2$, the resonance at −9.0 ppm, associated to cysteine 374, broadened to an extent that it could no longer be observed (Figure 1B). In contrast, the resonances of both labels attached to cysteine residues 10 and 285 are not appreciably modified following polymerization, as was observed by Brauer and Sykes (*18*).

Therefore, the results demonstrate that cysteines 10 and 285 are not significantly affected by actin polymerization, while cysteine 374 is greatly affected. The increase in the effective correlation time of the label attached to cysteine 374 is most likely due to a severe reduction of its mobility in F-actin. This could be due to a nonisotropic mobility of the F-actin filament or to an immobilization of cysteine 374 as a result of the interaction between actin monomers (*18, 19*). If this second hypothesis is true and considering the fact that labeling of cysteine 374 did not inhibit actin polymerization, this residue is most likely located not directly at the binding site, but rather close to it (*18, 19, 36, 37*).

Our results are also in agreement with a recent ^{1}H and ^{19}F NMR study indicating that the amino acids 1−22 are in a highly mobile state in Mg−F-actin (*22*). In addition, the ^{19}F NMR spectrum of actin specifically labeled at cysteine 374 obtained by Heintz et al. (*22*) indicates that the full line width at half-height $\Delta\nu_{1/2}$ is 19 Hz for Mg−G-actin, corresponding to a transverse relaxation time of 16.7 ms at 283 K. After polymerization, the line width $\Delta\nu_{1/2}$ is 520 ± 40 Hz, corresponding to a transverse relaxation time of 0.6 ms. This indicates a strong decrease of the mobility of cysteine 374 upon polymerization (*22*).

Interaction between G-Actin and Zwitterionic Liposomes. Figure 2 shows the ^{19}F NMR spectra of labeled G-actin in the presence of different types of liposomes. When G-actin is in the presence of zwitterionic liposomes made of pure DMPC (Figure 2A), the resonances of the labels attached to the three cysteines remain unaffected. Therefore, the interaction of labeled G-actin with zwitterionic liposomes does not change the environment of the three cysteine residues, suggesting that there is no interaction with actin. This is in agreement with the results of St-Onge and Gicquaud indicating that there is no interaction between G-actin and zwitterionic liposomes in the absence of divalent cations (*11, 12*).

We have also used ^{31}P and ^{2}H NMR to study the effect of actin on the conformation and order of the lipid headgroup. Figure 3A shows the ^{31}P NMR spectra at 30 °C of DMPC in the absence and presence of G-actin. These spectra indicate that a lamellar phase is obtained, both in the absence and in the presence of actin. Figure 4A shows the ^{2}H NMR spectra at 30 °C of the headgroup deuterated DMPC (DMPC-d_4) at the α and β positions, in the absence and in the presence of G-actin. Previous experiments (*26, 38*) have shown that the larger and the smaller quadrupolar splittings are respectively attributed to the α-CD_2 and β-CD_2 methylene of the choline moiety. In such cases, counterdirectional changes in the magnitudes of the α and β deuteron quadrupolar splittings have been observed in response to changes in membrane surface-charge density. The presence of a negative charge at the membrane surface has been shown to increase the α deuteron splitting and to decrease the β deuteron splitting, while the presence of a positive charge has the opposite effect.

The quadrupolar splittings for the two methylene groups are given in Table 1. In addition, Figure 5 shows the variation of the quadrupolar splittings for the α and β deuterons as a function of temperature. The addition of actin to pure DMPC-d_4 bilayers does not result in any change of either the α or β deuteron splittings, within experimental error. This indicates that there is no interaction between the negatively charged actin molecule and the DMPC headgroup. These results are in agreement with those previously obtained by electron microscopy and differential scanning calorimetry (*13*) and with the fact that the ^{19}F NMR spectrum of

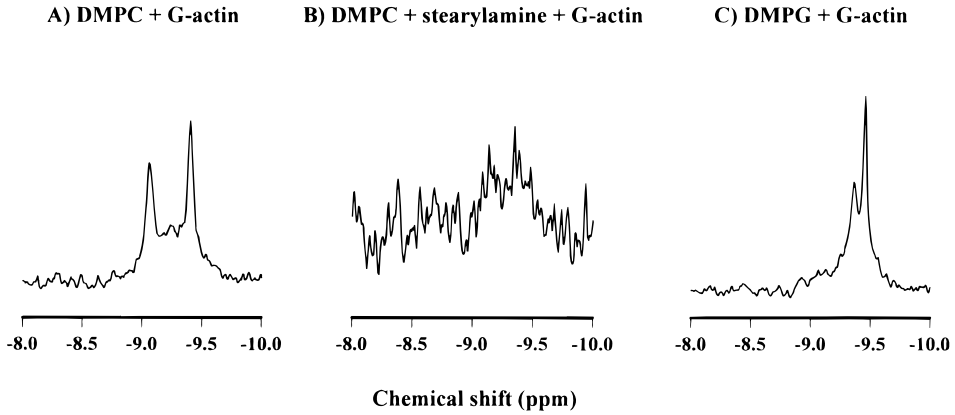

FIGURE 2: ^{19}F NMR spectra at 24 °C of labeled G-actin in the presence of (A) DMPC, (B) DMPC−stearylamine (9:1 molar ratio), and (C) DMPG.

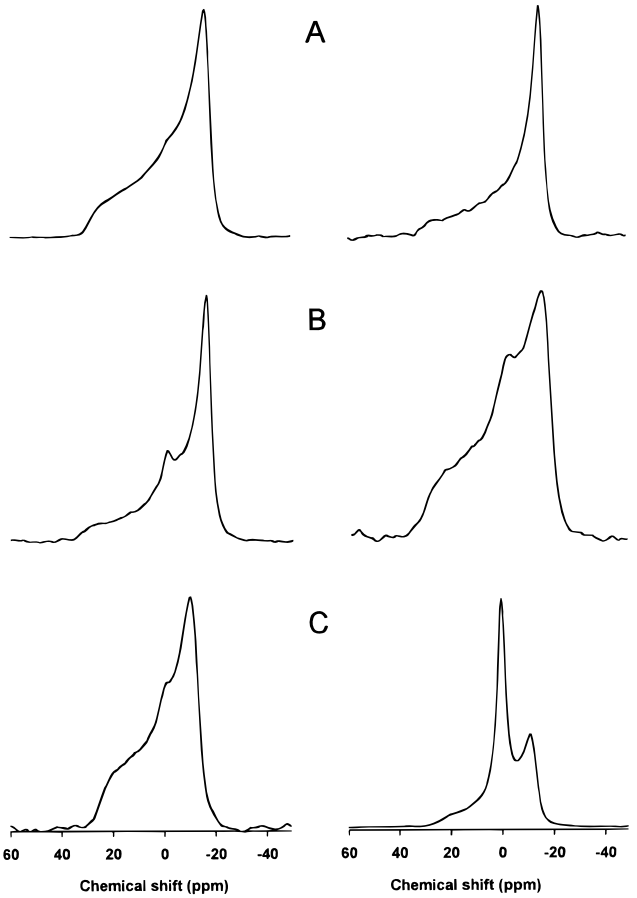

FIGURE 3: ^{31}P NMR spectra at 30 °C of (A) pure DMPC, (B) DMPC−stearylamine (9:1 molar ratio), and (C) DMPC−DMPG (1:1 molar ratio) in the absence (left) and in the presence (right) of G-actin.

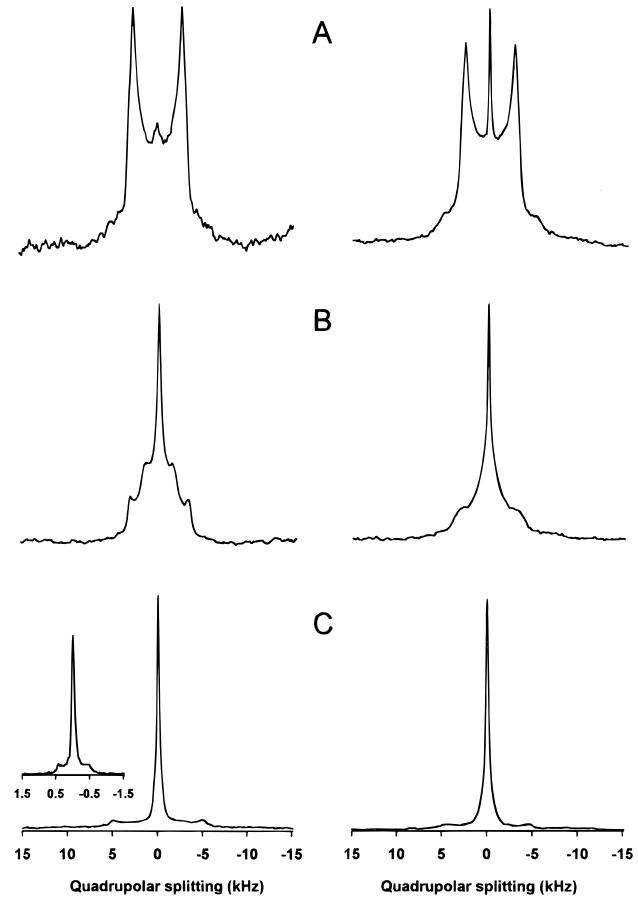

FIGURE 4: ^{2}H NMR spectra at 30 °C of headgroup deuterated DMPC at the α and β positions in the absence (left) and in the presence (right) of G-actin for (A) pure DMPC-d_4, (B) DMPC-d_4−stearylamine (9:1 molar ratio), and (C) DMPC-d_4−DMPG (1:1 molar ratio). The inset in Figure 4C (left) is the center part of the spectrum between 1.5 and −1.5 kHz, plotted with no line broadening in order to clearly distinguish the small quadrupolar splitting due to the β deuterons.

fluorinated G-actin is not modified in the presence of DMPC liposomes.

Interaction between G-Actin and Positively Charged Liposomes. Figure 2B shows that in the presence of positively charged liposomes, significant changes are observed in the ^{19}F NMR spectra of fluorinated G-actin. More specifically, the ^{19}F resonances associated with the three alkylated cysteine residues almost disappear, and only a weak signal can be observed around −9.3 and −9.4 ppm. The loss of intensity in the resonances of the labeled G-actin in the presence of positively charged liposomes can be explained by the strong electrostatic interactions between the anionic actin and positive stearylamine. This interaction may concentrate the monomers at the surface of the liposomes, inducing a complete reorganization of the conformation of actin in which the labels attached to the cysteines are then in an environment that reduces their mobility. These results are in agreement with those obtained by Gicquaud and Laliberté (*39*), who have demonstrated by electronic microscopy that when G-actin is in the presence of posi-

Table 1: Quadrupolar Splittings (in kHz) for Headgroup Deuterated DMPC-d_4 in the Systems DMPC, DMPC−Stearylamine (9:1 Molar Ratio), and DMPC−DMPG (1:1 Molar Ratio) in the Absence and Presence of Actin

T (°C)	DMPC	DMPC + actin	DMPC−SA	DMPC−SA + actin	DMPC−DMPG	DMPC−DMPG + actin
				α Deuterons		
25	6.10	6.15	4.18	7.15	10.62	10.23
30	6.26	6.20	3.49	7.28	10.38	9.81
35	6.30	6.23	3.52	7.08	10.33	9.62
40	6.13	6.25	3.47	6.91	10.35	9.38
				β Deuterons		
25	6.10	6.15	6.62	2.78	1.00	1.88
30	5.69	5.76	6.67	2.66	0.93	1.54
35	5.25	5.34	6.32	2.66	0.73	1.12
40	4.91	5.00	6.01	2.66	0.59	0.83

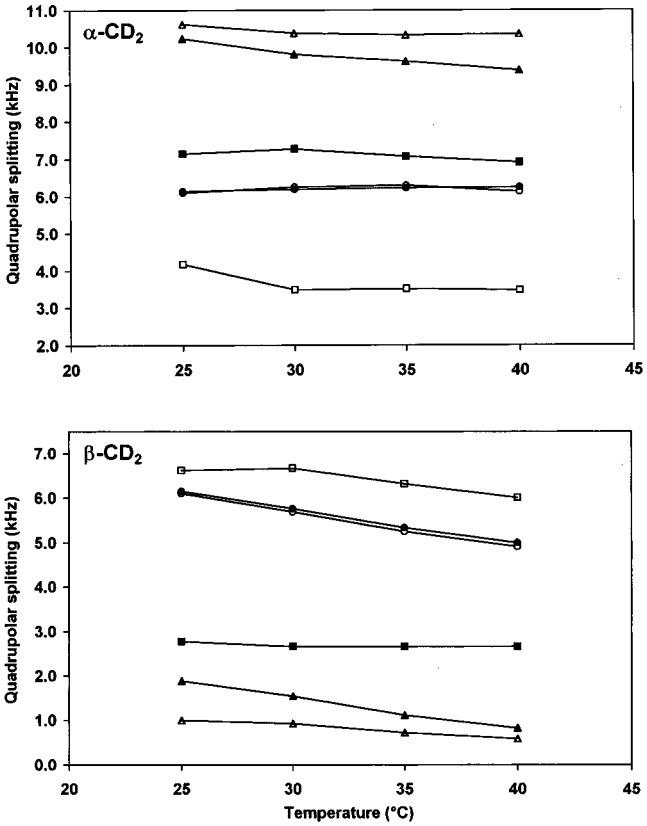

FIGURE 5: Quadrupolar splittings as a function of temperature for the α and β deuterons of DMPC-d_4 in the absence (open symbols) and presence (filled symbols) of G-actin for pure DMPC-d_4 (●), DMPC-d_4−stearylamine (9:1 molar ratio) (■), and DMPC-d_4−DMPG (1:1 molar ratio) (▲).

tively charged liposomes made of phosphatidylcholine and stearylamine, the conformation of actin is modified. In fact, it was shown that the interaction of G-actin with positively charged liposomes induces polymerization of the protein.

Examination of the preparation by electron microscopy (Figure 6A) shows that G-actin organizes with the DMPC−stearylamine mixture in aggregates which are several micrometers in size. Figure 6A illustrates one of these aggregates. One can see that it is made of densely packed parallel actin filaments. It is clear from this observation that the DMPC−stearylamine mixture induces the polymerization of actin since actin in G buffer is not normally polymerized. These results are in agreement with the ^{19}F NMR spectrum of this system shown in Figure 2B, which indicates a complete immobilization of the actin molecules, at least at the sites of the cysteine residues 10, 285, and 374 in the presence of DMPC−stearylamine.

We have also investigated the interaction between G-actin and positively charged liposomes using ^{31}P and ^{2}H NMR solid-state NMR spectroscopy. Figure 3B shows the ^{31}P NMR spectra obtained for the DMPC−stearylamine system, both in the absence and in the presence of actin. These results show in both cases the presence of a small isotropic peak superimposed to a lamellar phase spectrum. The isotropic peak could be due to the formation of a small number of rapidly tumbling vesicles, but the large proportion of lamellar phase spectra indicates that the presence of 10% stearylamine does not perturb significantly the lamellar structure of the DMPC bilayers. Neither is this lamellar phase significantly affected by the presence of actin.

Figure 4B shows the ^{2}H solid-state NMR spectra of DMPC-d_4−stearylamine (9:1 molar ratio) in the absence and presence of actin. The isotropic peaks observed in the center of these spectra are most likely due to a combination of residual ^{2}H in the G buffer and to the presence of a small number of rapidly tumbling vesicles, as indicated by the ^{31}P NMR spectra. Upon addition of stearylamine, a positively charged surfactant, the splitting that has been attributed to the α-CD_2 group in pure DMPC-d_4 increases while the splitting attributed to the β-CD_2 group decreases. This behavior is unexpected for the addition of a positively charged molecule close to the DMPC headgroup, which has been shown to result in a decrease of the α deuteron splitting with a concomitant increase of the β deuteron splitting (*40*). However, if we attribute the smaller splitting observed in the presence of 10% stearylamine to the α-CD_2 group and the larger splitting to the β-CD_2 group, the α splitting decreases from 6.26 to 3.49 kHz and the β splitting increases from 5.69 to 6.67 kHz in the presence of stearylamine at 30 °C. These changes are in the direction expected for cationic surface charges, and their magnitudes are as well (*40*).

The addition of G-actin to the positively charged DMPC-d_4−stearylamine liposomes results in an increase of the α deuteron splitting with a concomitant decrease of the β deuteron splitting (Figure 5 and Table 1). At 30 °C, the α splitting increases from 3.49 to 7.28 kHz in the presence of actin while the β splitting decreases from 6.67 to 2.66 kHz with the protein. This behavior is consistent with the interaction of the DMPC−stearylamine bilayers with a negative charge at the surface and is in agreement with the ^{19}F NMR and electron microscopy results, indicating a polymerization of the negatively charged actin molecules at the surface of the positively charged liposomes.

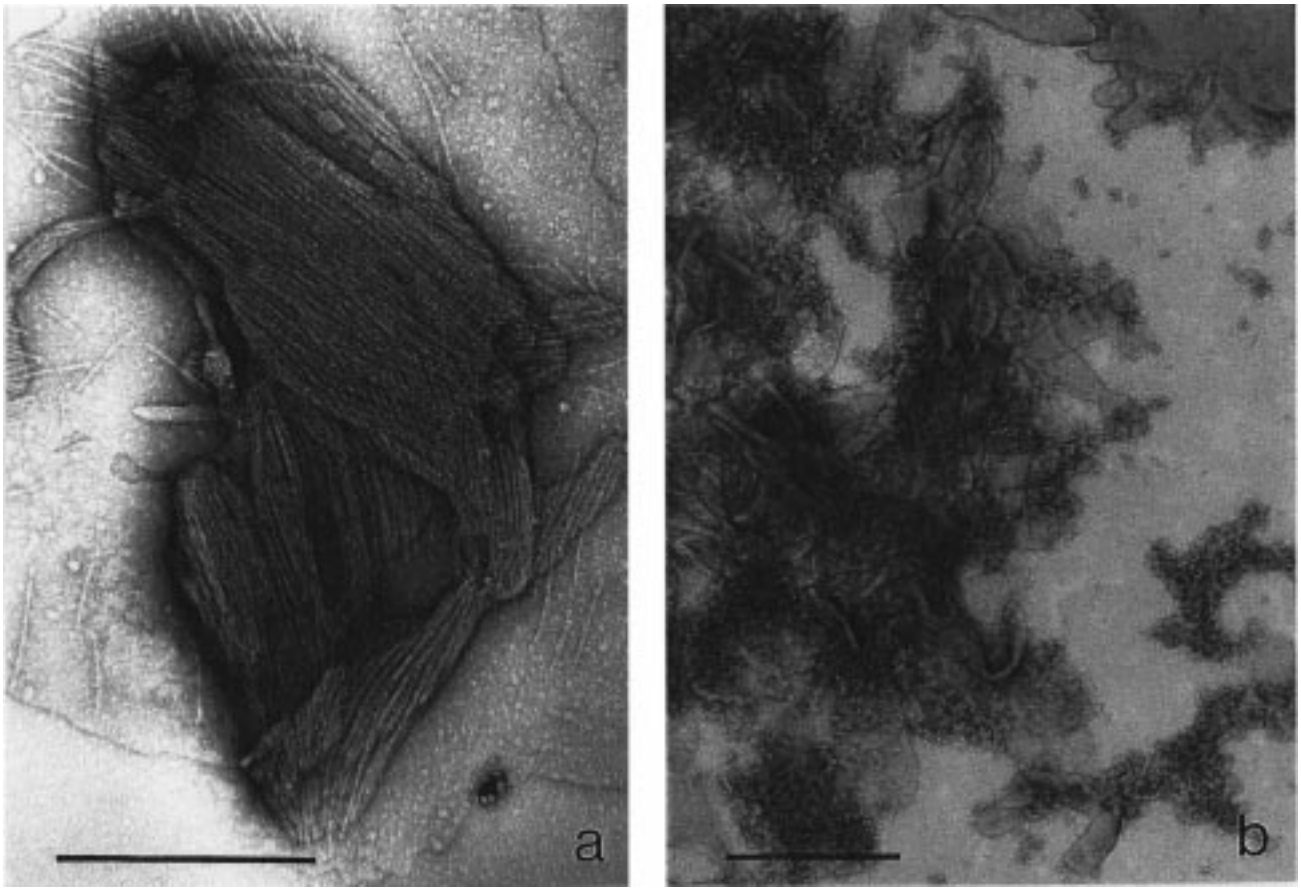

FIGURE 6: Electron micrographs of negatively stained mixtures of actin and (A) DMPC−sterarylamine (9:1 molar ratio) and (B) DMPG after 1 h of incubation. Bar = 0.5 μm.

Interaction between G-Actin and Negatively Charged Liposomes. Figure 2C presents the ^{19}F NMR spectrum of labeled G-actin in the presence of negatively charged DMPG liposomes. This spectrum indicates that when G-actin is in the presence of negatively charged liposomes, the peak associated with the label attached to cysteine 374 is not observed and the two remaining resonances are not significantly affected. This behavior is very similar to that obtained for pure polymerized F-actin. This therefore suggests an interaction between the actin molecule and the negatively charged liposomes, which could be associated with actin polymerization.

However, examination of the preparation by electron microscopy shows lipid vesicles and micelles of various sizes and morphologies (Figure 6B). It is clear from this figure that actin is not polymerized but appears as monomers uniformly distributed in the preparation. However, it is not possible to conclude from this picture that there is an interaction between actin and DMPG, but one cannot exclude that this interaction exists since if this interaction does not result in a polymerization or a paracrystallization of the actin molecules, it will be difficult to see on the electron micrographs.

Since actin is an anionic protein, its interaction with negatively charged liposomes is somewhat surprising. However, it is interesting to note that the three residues preceding cysteine 374 (His-Arg-Lys) are basic residues. The interaction of G-actin with DMPG could therefore be the result of an electrostatic interaction between these residues and DMPG. The close proximity of the fluorinated probe to the interacting residues would then rigidify the environment of the label, which would explain the complete broadening of the resonance of cysteine 374 in the presence of DMPG.

We have also investigated the interaction between G-actin and negatively charged liposomes made of DMPC−DMPG (1:1 molar ratio) using ^{31}P and ^{2}H NMR solid-state NMR spectroscopy. The presence of deuterated DMPC was necessary in the ^{2}H NMR experiments as a probe for the molecular voltmeter effect. The assumption is made, however, that the interaction of actin with the DMPG molecules would affect the DMPC headgroup enough to give rise to a change in the ^{2}H quadrupolar splittings.

The ^{31}P NMR spectrum obtained for the DMPC−DMPG system in the absence of actin (Figure 3C, left) is typical of a lamellar phase, and only a small isotropic peak is detected in the system. For the DMPC−DMPG−actin system (Figure 3C, right), the results show the presence of a large isotropic peak in the ^{31}P spectrum, which accounts for about 45% of the total spectrum. These results are in agreement with those obtained by electron microscopy, which suggest the formation of vesicles of various sizes and morphologies for the DMPC−DMPG system in the presence of actin.

Figure 4C shows the ^{2}H solid-state NMR spectra of DMPC-d_4−DMPG (1:1 molar ratio) in the absence (left) and the presence (right) of actin. The small quadrupolar splitting, associated with the β-CD_2 group, is difficult to observe in the spectra plotted with a 200 Hz line broadening, but is easily seen in the spectra with no line broadening, as shown on the inset in Figure 4C. This inset also clearly indicates that the center peak in the spectrum is due to both an isotropic

peak and a powder pattern with a very small quadrupolar splitting. Since the ^{31}P NMR spectrum of this system is typical of a lamellar phase, the central peak obtained in the ^{2}H NMR spectrum is due mostly to residual ^{2}H in the buffer. The addition of DMPG to DMPC-d_4 bilayers results in a large increase of the α deuterons and in a large decrease of the β deuterons (Figure 5 and Table 1). This behavior is consistent with the addition of a negative charge close to the DMPC headgroup (*40*).

The addition of G-actin to the DMPC-d_4−DMPG system has the opposite effect (Figure 4C, right). It results in a small decrease of the α deuteron splitting with a concomitant increase of the β deuteron splitting (Figure 5 and Table 1). At 30 °C, the α splitting decreases from 10.38 to 9.81 kHz in the presence of actin while the β splitting increases from 0.93 to 1.54 kHz with the protein. As mentioned above, this behavior is characteristic of the proximity of a positive charge close to the DMPC headgroup. This result is in agreement with an interaction of the actin molecule with the three positive charges (His-Arg-Lys) located just before the cysteine residue 374 in the protein, as suggested by the strong broadening of the cysteine 374 resonance observed in the ^{19}F NMR spectrum of the actin−DMPG complex. However, since a heterogeneous vesicle population is observed for this system, by both electron microscopy and ^{31}P solid-state NMR, the ^{2}H NMR results could also suggest that actin preferentially segregates a population of DMPG into small vesicles, leaving the DMPC large vesicles partially depleted of DMPG and displaying the observed splittings.

CONCLUSION

The results of the present study strongly indicate that the monomeric actin molecule is interacting with both positively and negatively charged liposomes, while there is no evidence of interaction with zwitterionic liposomes. More specifically, the ^{19}F NMR spectroscopy results indicate that the mobility of cysteines 10, 285, and 374 is significantly decreased when actin is in the presence of positively charged liposomes. This result is confirmed by electron microscopy, indicating the formation of actin filaments at the surface of the liposomes. On the other hand, the ^{19}F, ^{31}P, and ^{2}H NMR results indicate an interaction between actin and negatively charged liposomes. This result, somewhat surprising, could be explained by an interaction between the three positively charged residues (His-Arg-Lys) preceding cysteine 374 in the actin primary sequence. Since natural membranes contain a large proportion of negatively charged lipids, the demonstration of an interaction between actin and negatively charged lipids could bring some insights on the interaction between actin and membranes in vivo.

ACKNOWLEDGMENT

The authors thank Dr. Pierre Tancrède for several helpful discussions and Mr. Guillaume Grenier for the preparation of unlabeled actin.

REFERENCES

1. Pantaloni, D., Terrell, L. H., Carlier, M. F., and Korn, E. D. (1985)*Proc. Natl. Acad. Sci. U.S.A. 82*, 7207−7211.
2. Wuestehube, L., and Luna, E. (1987) *J. Cell Biol. 105*, 1741−1751.
3. Korn, E. D., and Hammer, J. (1990) *Curr. Opin. Cell Biol. 2*, 57−61.
4. Scheel, J., Ziebelbauer, K., Kupke, T., Humbel, B., Noegel, A., Gerish, G., and Schleicher, M. (1989) *J. Biol. Chem. 264*, 2832−2839.
5. Bennet, V. (1989) *Biochim. Biophys. Acta 988*, 107−121.
6. Bennet, V. (1984) in *Cell Membrane: Methods and Reviews* (Elson, E., Ed.) pp 149−195, Plenum Press, New York.
7. Rotman, A., Heldman, J., and Linder, S. (1982) *Biochemistry 21*, 1713−1719.
8. Otto, J. (1990) *Cell Motil. Cytoskeleton 16*, 1−6.
9. Burridge, K., and Cornell, L. (1983) *Cell Motil. 3*, 405−417.
10. Rioux, L., and Gicquaud, C. (1985) *J. Ultrastruct. Res. 93*, 42−49.
11. St-Onge, D., and Gicquaud, C. (1989) *Biochem. Cell Biol. 67*, 297−300.
12. St-Onge, D., and Gicquaud, C. (1990) *Biochem. Biophys. Res. Commun. 167*, 40−47.
13. Gicquaud, C. (1993) *Biochemistry 32*, 11873−11877.
14. Gicquaud, C., and Wong, P. T. T. (1994) *Biochem. J. 303*, 769−774.
15. Kabsch, W., and Vandekerckhove, J. (1992) *Annu. Rev. Biophys. Biomol. Struct. 21*, 49−76.
16. Vandekerckhove, J., and Weber, K. (1979) *Differentiation 14*, 123−133.
17. Korn, E. D. (1982) *Physiol. Rev. 62*, 672−737.
18. Brauer, M., and Sykes, B. D. (1986) *Biochemistry 25*, 2187−2191.
19. Barden, J. A., Phillips, L., Cornell, B. A., and dos Remedios, C. G. (1989) *Biochemistry 26*, 5895−5901.
20. Lusty, C. J., and Fasold, H. (1969) *Biochemistry 8*, 2933−2939.
21. Gerig, J. T. (1978) *Biol. Magn. Reson. 1*, 139−203.
22. Heintz, D., Kany, H., and Kalbitzer, H. R. (1996) *Biochemistry 35*, 12686−12693.
23. Sixl, F., and Watts, A. (1983) *Proc. Natl. Acad. Sci. U.S.A. 80*, 1613−1615.
24. Seelig, J., Macdonald, P. M., and Scherer, P. G. (1987) *Biochemistry 26*, 7535−7541.
25. Roux, M., Neumann, J., Hodges, R. S., Devaux, P., and Bloom, M. (1989) *Biochemistry 28*, 2313−2321.
26. Scherer, P. G., and Seelig, J. (1987) *EMBO J. 6*, 2915−2922.
27. de Kroon, A., Killian, J. A., de Gier, J., and de Kruijff, B. (1991) *Biochemistry 30*, 1151−1162.
28. Marassi, F. M., and Macdonald, P. M. (1991) *Biochemistry 30*, 10558−10566.
29. Marassi, F. M., and Macdonald, P. M. (1992) *Biochemistry 31*, 10031−10036.
30. Macdonald, P. M. (1997) *Acc. Chem. Res. 30*, 196−203.
31. Spudich, J., and Watts, S. (1971) *J. Biol. Chem. 246*, 4866−4871.
32. Nonomura, Y., Katayama, E., and Ebashi, S. (1975) *J. Biochem. (Tokyo) 78*, 1101−1104.
33. Davis, J. H., Jeffrey, K. R., Bloom, M., Valic, M. I., and Higgs, T. P. (1976*) Chem. Phys. Lett. 42*, 390−394.
34. Bloom, M., Davis, J. H., and MacKay, A. L. (1981) *Chem. Phys. Lett. 80*, 198−202.
35. Sternin, E., Bloom, M., and MacKay, A. L. (1983) *J. Magn. Reson. 55*, 274−282.
36. Elzinga, M., and Phelan, J. J. (1984) *Proc. Natl. Acad. Sci. U.S.A. 81*, 6599−6602.
37. Sutoh, K. (1984) *Biochemistry 23*, 1942−1946.
38. Gally, H.-U., Niederberger, W., and Seelig, J. (1975) *Biochemistry 14*, 3647−3652.
39. Gicquaud, C., and Laliberté, A. (1988) *J. Cell Biol. 106*, 1221−1227.
40. Scherer, P. G., and Seelig, J. (1989) *Biochemistry 28*, 7720−7728.

BI971892R